RSC Advances

ROYAL SOCIETY OF CHEMISTRY

www.rsc.org/advances

Preparation of highly permeable alumina membrane via wet film phase inversion

Wu Qin, Cheng Peng, Jianqing Wu[ξ]

Wet film phase inversion technique has been applied for the single-step preparation of alumina membrane for the first time. During the phase inversion process of cellulose acetate (CA), orientated microtubular pores were formed and the membrane with narrow pore size distribution, good connectivity and small tortuosity was achieved on the as-prepared macroporous ceramic support. The membrane prepared using the slurry with α-Al_2O_3/CA ratio of 15.83/4.17 exhibited a pore size distribution centered at about 0.28 μm and a water permeance of 1327 L m^{-2} h^{-1} bar^{-1}.

Ceramic membranes are usually constituted by several layers of one or more kinds of ceramic materials. [1] They are generally prepared in a multilayered structure with progressively decreasing pore sizes from the macroporous support to the effective filtration layer. [2, 3] The substrate provides mechanical support, and one or a few of middle layers bridge the pore size differences between the substrate and the effective filtration top layer. [4, 5, 6] However, the shortcoming of the multilayered structure is not only to bring about the increase of membrane thickness and cause the sharp ascent of filtration resistance, but

School of Materials Science and Engineering, South China University of Technology, Guangzhou 510640, China.

E-mail address: imjqwu@scut.edu.cn; Tel: +86-20-87111669; fax: +86-20-87110273.

also to increase preparation procedures, time and cost. Each step of the multiple coating processes involves a high temperature treatment process, making the ceramic membrane fabrication extremely expensive.

The phase inversion process was originally developed for preparation of polymer membranes .[7-9] Recently, this technique has been developed for the integrated preparation of ceramic membranes constituted of the support layer and the separation layer, such as the ceramic hollow fiber membranes. [10-21] In this study, wet film phase inversion technique has been developed only for the ceramic membrane top layer. The viscosity of membrane coating slurry is adjusted to a proper value according to our previous work. [22] The membrane with high pore connectivity, narrow pore size distribution and low filtration resistance has been achieved by taking advantage of the phase inversion of cellulose acetate.

Disc alumina supports with the sizes of 25 mm in diameter and 3 mm in thickness were prepared based on our earlier work. [4] The support has an open porosity of 47.8%, a water permeance of 3650 L m^{-2} h^{-1} bar^{-1}, an average pore size of 2.1 μm as well as the flexural strength of 68.7 MPa. A powder mixture consisting of boehmite (1.7 wt%) (AlOOH) (99.9%, D_{50} = 40 nm, Tianjin Boyuan New Materials Co., Ltd, China) and 15 wt% ~ 17.5 wt% alumina (α-Al_2O_3) (99.99%, d_{50} = 100 nm, Taimei Chemicals Co., Ltd. Nagno-ken, Japan) was dispersed in N,N-dimethyl formamide (77.4 wt%) (DMF) (AR, Shanghai Richjoint Chemical Reagent Co., Ltd, China) and milled for 2 h at room temperature with a planetary mill. Subsequently, cellulose acetate (2.5 wt% ~ 5 wt%)(CA) (Shanghai Richjoint Chemical

Reagent Co., Ltd, China) and Polyvinyl Pyrrolidone (0.9 wt%)(PVP)(K30, Shanghai Yuanju Biological Technology Co., Ltd, China) were added in this mixture then stirred for 24 h. After the as-obtained ceramic slurry was degassed at room temperature for more than 30 min, the supports whose one face had been sealed by masking tape were dip coated in the slurry at a withdrawal speed of 5 mm/s [23]. The coated supports were immediately immersed in water at room temperature and kept for 30 min for the phase inversion from liquid to solid. After drying under ambient conditions, the green membranes were heated at a rate of 2 ℃ /min to 500℃, maintained at that temperature for 1 h to remove the polymers, followed by sintering at 1200℃ for 2 h in air. The samples were cooled down to room temperature naturally.

The phase inversion process of membrane formation is mainly affected by the specific thermodynamic situation, the interactions among the constituents and kinetic factors [24]. According to Barton's [25] and Boom's [26] works, the phase inversion process can be investigated by means of the phase diagram of water-DMF-cellulose acetate system (see Fig. 1). When the wet film was inserted into water, the inter-diffusion between water and the solvent DMF took place immediately. The DMF concentration on the membrane surface would decrease sharply at the moment to contact with water and the phase separation process was triggered. Due to the high concentration gradient of CA at the interface between water and wet film, the composition of polymer solution moved from A to B (Fig. 1) and reached the glass transition line directly [27], followed by the formation of a homogeneous and dense glassy-state layer. Alumina particles on the wet film surface were

absorbed and fixed in situ by precipitated cellulose acetate and instantaneously formed a skin layer with uniformly distributed thin pores (Fig. 2(a)). Under the cured surface, the inter-diffusion rate gradually decreased as the depth increased. The component of polymer solution moved along the A-C line and enter the metastable region. The phase separation change smoothly from spinodal deposition to nucleation and growing process until glass transition. The polymer-rich phase was solidified when reaching the glass transition line; the polymer-lean phase nucleated and grew up forming pores under surface tension [28]. The cellulose acetate dissolved in DMF might diffuse to the solid phase CA and grow to fibers orienting toward skin layer along with the inward phase inversion reaction (Fig. 2(d)). The pores resulted from the nucleation and growth of polymer-lean phase were filled with alumina particles. Following the phase inversion of CA alumina particles were ‘solidified’ in the membrane. Fig. 2 roughly describes the evolution process. During sintering, the orientated fibers were burned out and formed a lot of microtubular channels and the membrane with good connectivity and small tortuosity were achieved.

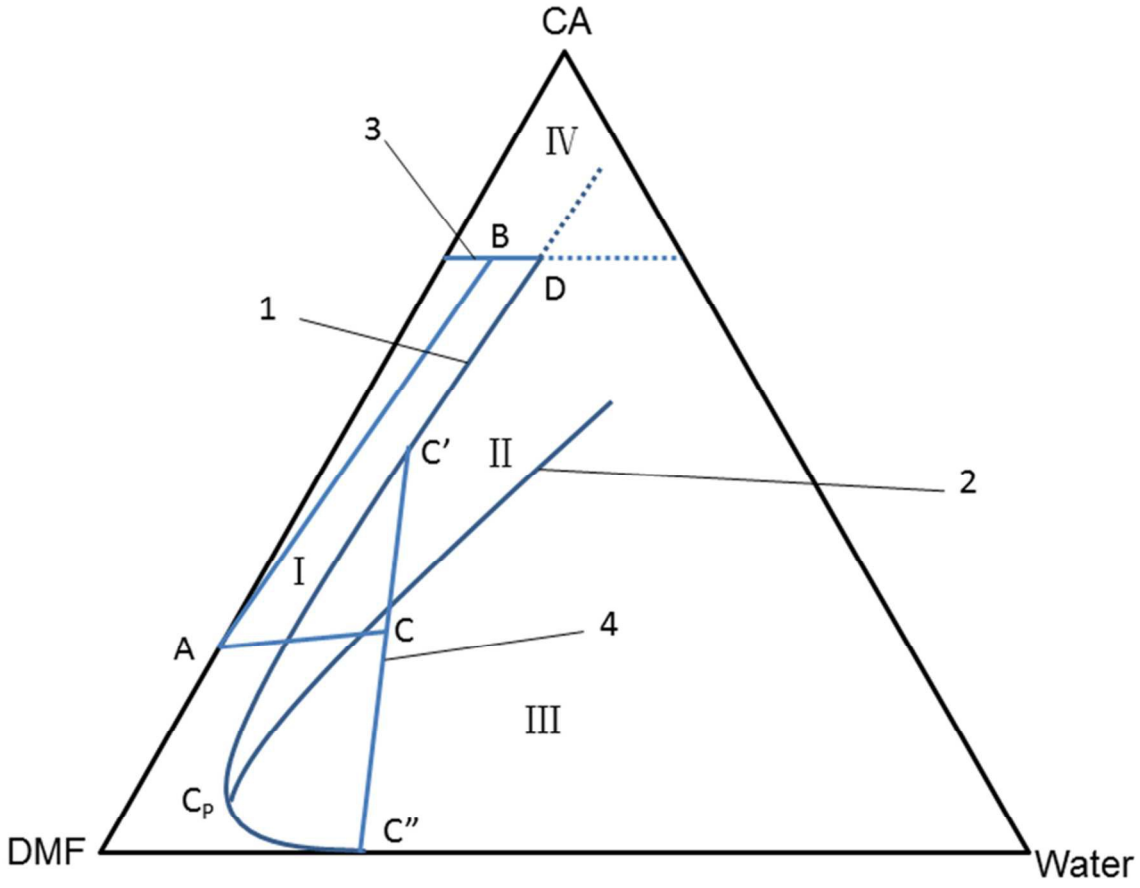

Fig. 1. Phase diagram of water-DMF-cellulose acetate system. 1 - binodal; 2 - spinodal; 3 - glass transition line; 4 - tie-line; I - single-phase solution region; II – metastable region; III – instable region; IV – glass transition region; C' – polymer-rich phase; C" – polymer-lean phase.

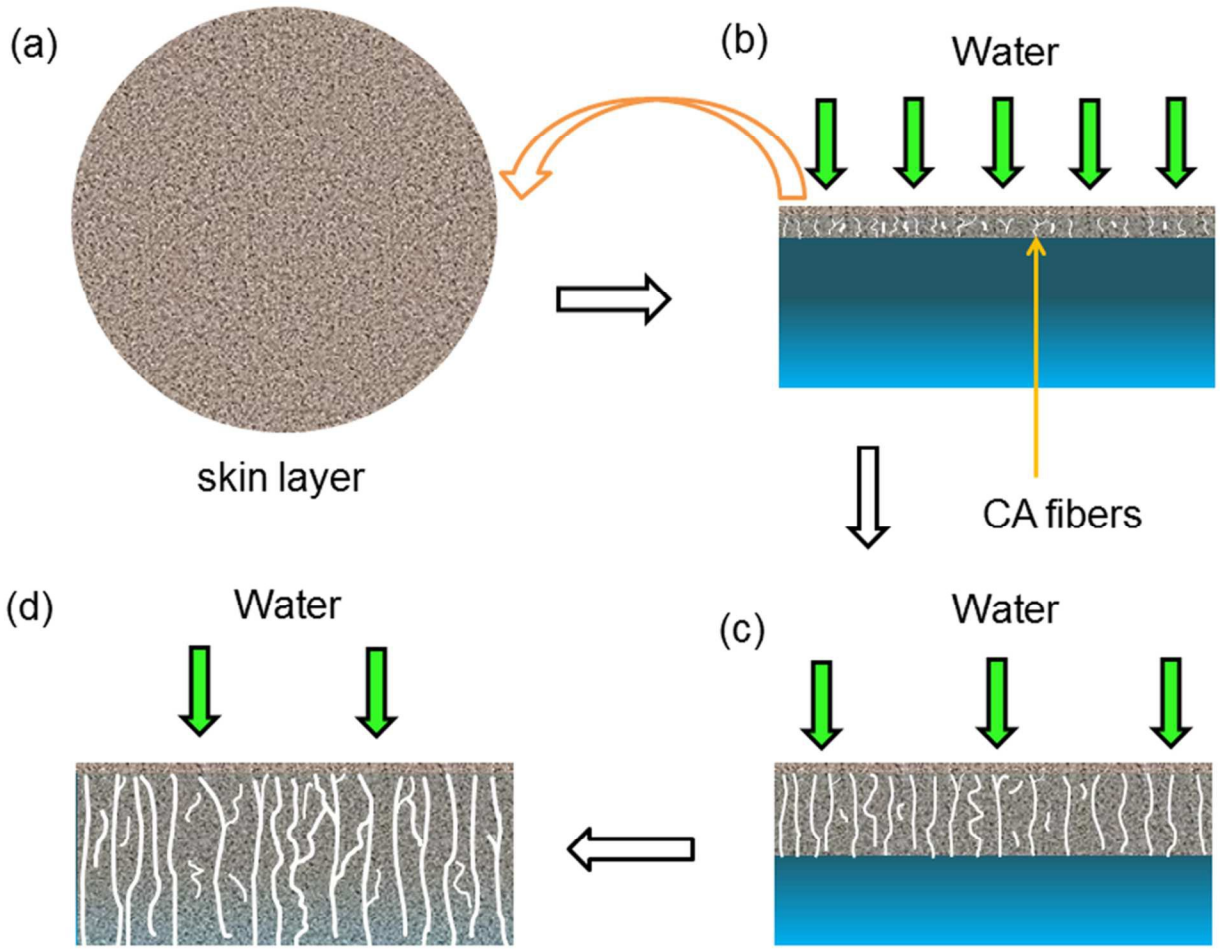

Fig. 2. Schematic depiction of the orientated microtubular pore structure formation process in the membrane: (a) phase inversion triggered immediately and a skin layer formed instantaneously on the wet film surface hardly when the wet film contact with water; (b) under the cured skin layer, the dissolved cellulose acetate diffused to the solid CA and grew to fibers, and the inter-diffusion rate decreased as depth increased; (c, d) CA fibers grew up orienting toward skin layer along with the inward phase inversion reaction.

As shown in Fig. 3, the XRD patterns of the final membrane product can be exclusively indexed to α-Al_2O_3 phase according to JCPDS 37-1462. The morphology of the

synthesized membrane was characterized with SEM. Fig. 4 presents the typical membrane microstructures before and after sintering. No any cracks or other defects can be observed in the surface of the dried green membrane (Fig. 4a). Fig. 4(b) shows the surface after sintering, alumina particles were dispersed uniformly in the membrane. Fig. 4(c) is the cross-sectional morphology of the prepared membrane. From the partial magnified image (Fig. 4(d)) orientated microtubular pore structures are clearly visible which makes the membrane has a small tortuosity and good connectivity. [29]

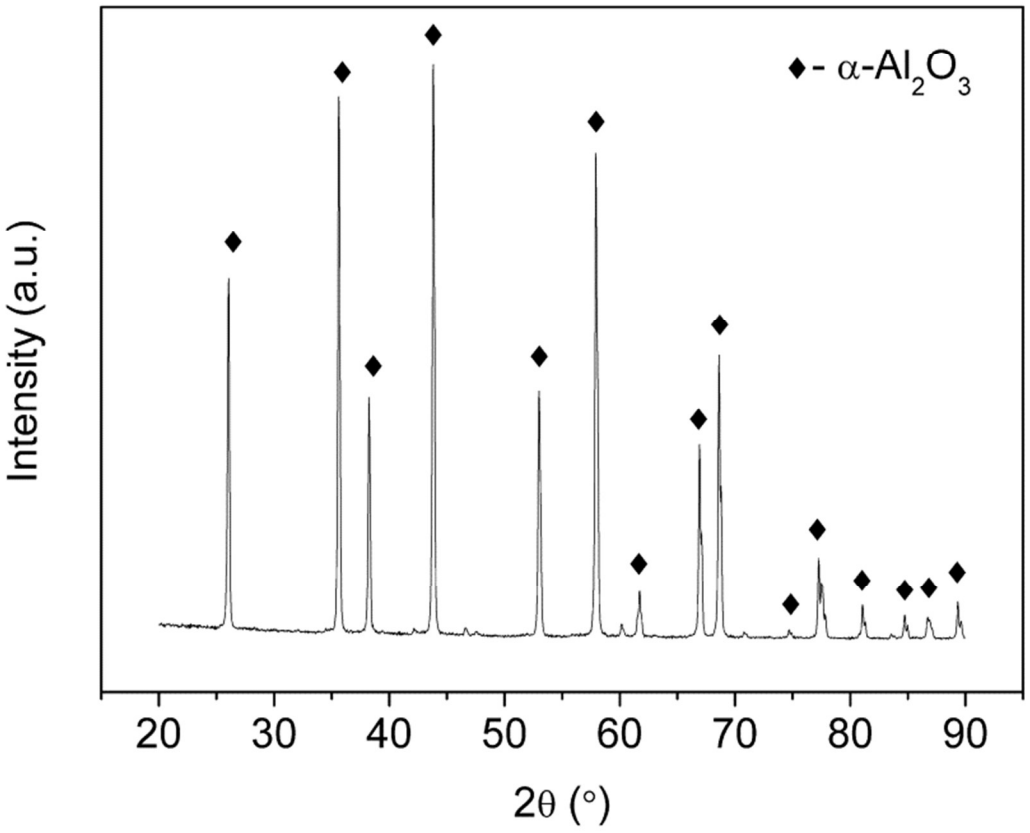

Fig. 3. XRD pattern of the final alumina membrane product.

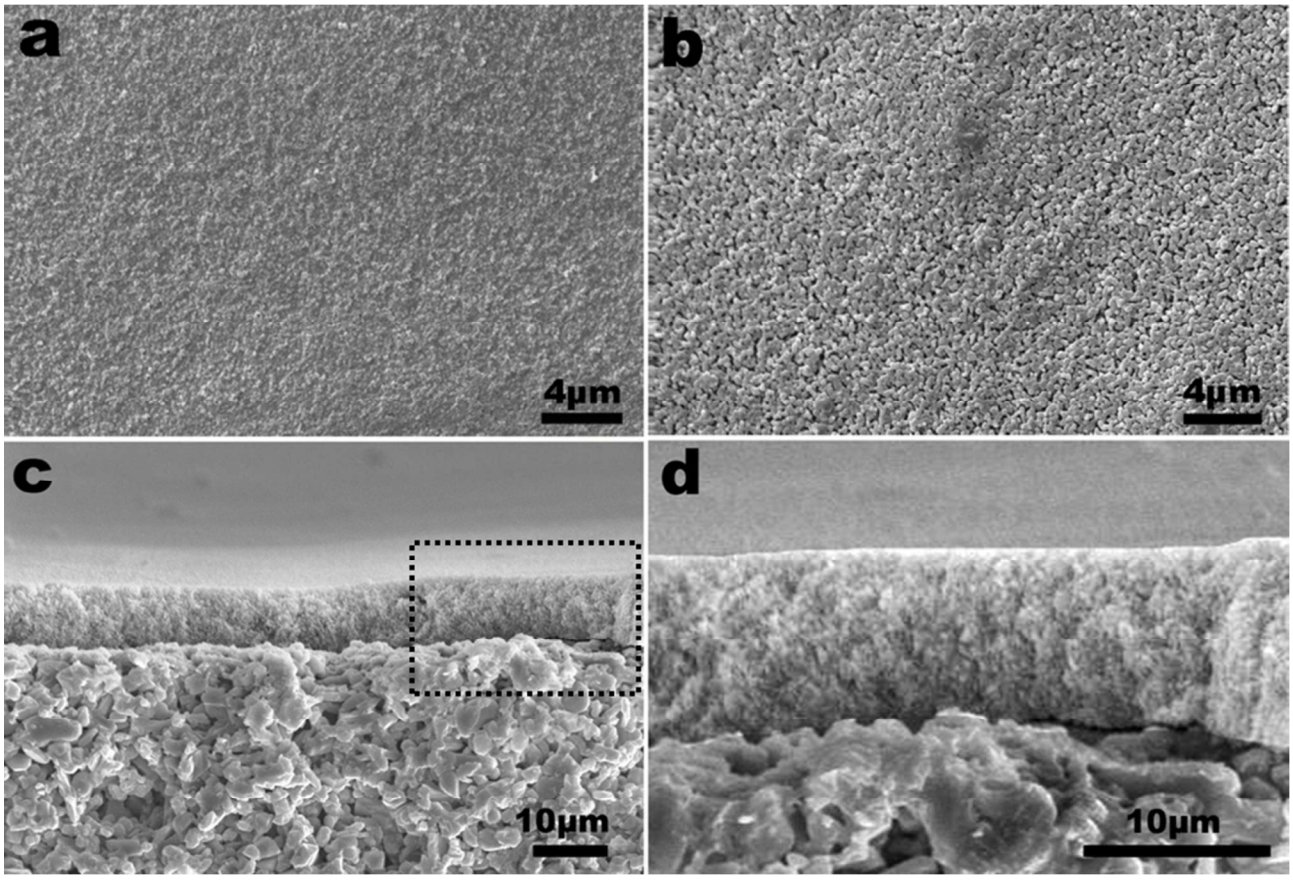

Fig. 4. SEM micrographs of the green membrane surface (a) and the membrane sintered at 1200℃: (b) sintered membrane surface; (c) sintered membrane cross-section; (d) partial magnified image of (c). [the slurry consists of 1.7 wt% AlOOH, 15.83 wt% α-Al_2O_3, 4.17 wt% CA, 77.4 wt% DMF and 0.9 wt% PVP].

Pore size distributions of the membranes were obtained by the gas bubble pressure method which was performed according to ASTM Publication F316-03(2011). All samples were immersed in anhydrous ethanol for 3 h under vacuum. The relationship between the nitrogen flow rate and the pressure difference at 27℃ is illustrated in Fig. 5. The gas flow of wet membrane emerges at the pressure difference of 2.99 bar which corresponds to the maximum pore size of 0.29 μm. As the pressure difference increases, more pores are

opened and the gas flow increases nonlinearly. When the pressure difference is increased to 3.41 bar, the gas flow increases sharply, indicating the most frequent pore size of the membrane is about 0.25 μm. After all of the wet pores are opened, the gas flow increases linearly with pressure difference according to the Hagen-Poiseuille equation. Cellulose acetate as a main film former exists in the green membrane, the weight ratio of α-Al_2O_3/CA has obvious influence on the pore size distributions of the membrane. Fig. 6 shows all membranes have a narrow pore size distribution. The average pore size and maximum pore size of the membranes increase with elevation of the relative amount of CA. The more the space of green ceramic membrane was occupied by CA, the bigger the average pore size formed.

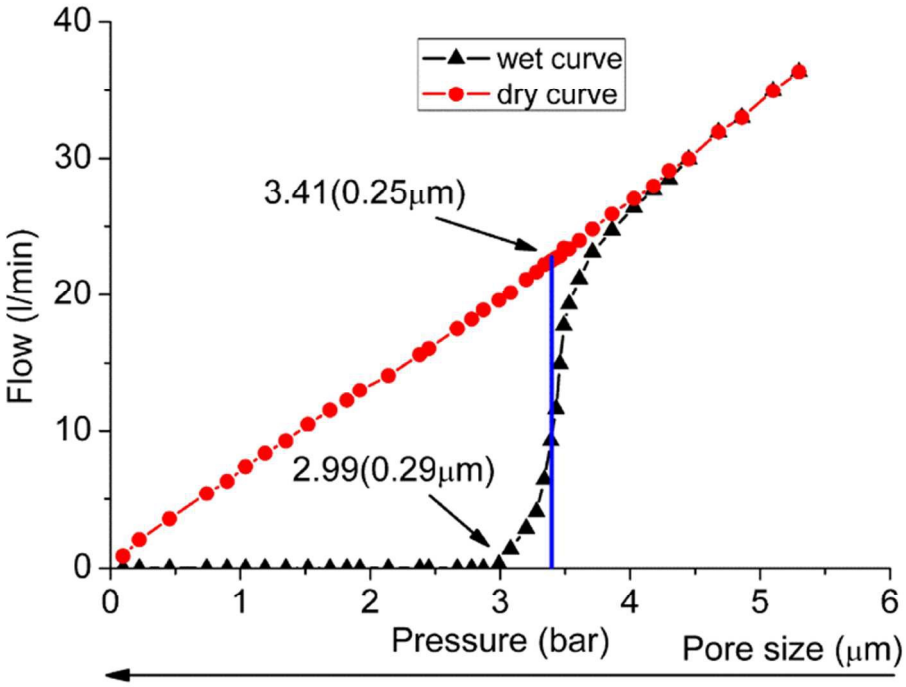

Fig. 5. The nitrogen flow rate through the wet (▲) and dry (●) membrane prepared using the slurry with α-Al_2O_3/CA ratio of 17.5/2.5.

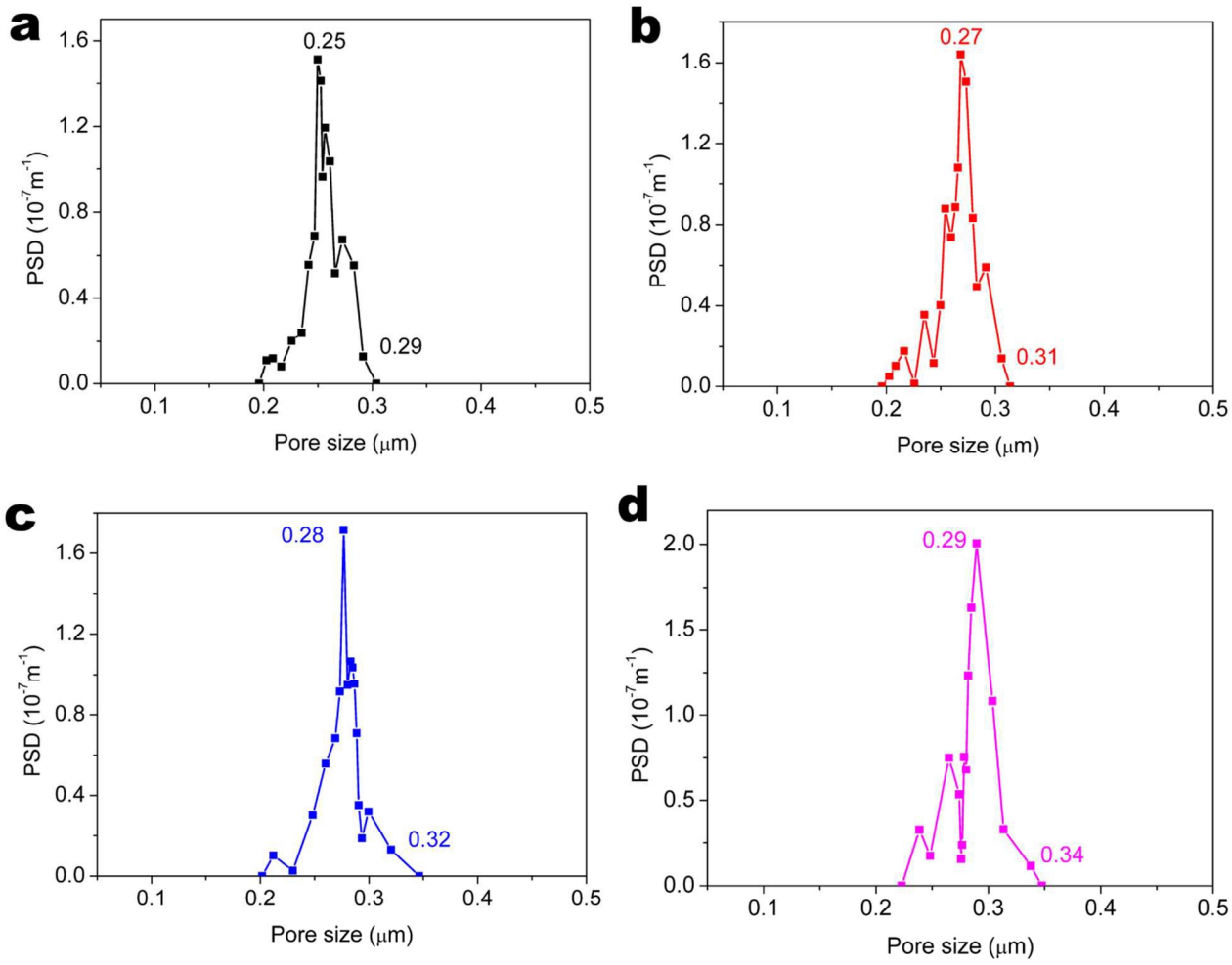

Fig. 6. Pore size distributions of the membranes prepared using slurries with different weight ratios of α-Al_2O_3/CA: (a) 17.5/2.5; (b) 16.67/3.33; (c) 15.83/4.17; (d) 15/5.

Water permeance of the membrane was tested on a Fully Automated Fluid and Gas Handling Systems OSMO Inspector 2.0 (Poseidon, Convergence, Netherlands). To avoid non-stationary transient effects, the membranes were saturated with deionized water (18 MΩ) before the pressure was applied. The effective filtration area of each sample was 2.545×10^{-4} m^2 by measurement and calculation. Viscosity of the slurry would affect the intrusion of the slurry into the support by capillary action and membrane thickness. The

higher the slurry viscosity the less the intrusion of the slurry into the support and the thicker the membrane. At a constant dip coating rate this increase of green membrane thickness is expected based on the physics of dip coating [30]. The filtration capacity of membrane will decrease as the increase of the intrusion of slurry into the support and the membrane thickness, vice versa [22]. Therefore as the viscosity varies a permeance peak would be found. Actually the thickness of the green membranes increases from 7 μm to 16 μm when the viscosity of the slurries increases from 262 mPa s to 572 mPa s. Fig. 7 presents the effects of weight ratios of α-Al_2O_3/CA on the membrane thickness, slurry viscosity and the membrane water permeance. When α-Al_2O_3/CA is 15.83/4.17, the water permeance reaches the peak value of 1327 L m^{-2} h^{-1} bar^{-1}; but when α-Al_2O_3/CA reaches 15/5 the permeance decreases to 1189 L m^{-2} h^{-1} bar^{-1} drastically instead. As the alumina/CA weight ratio decreases there is more CA in the green membrane and hence the pore content in the sintered membrane increases (which increases permeance), but the thickness also increases (which decreases permeance). When the CA content is more than 4.17 wt%, the effect of thickness increase is likely to surpass the effect of pore content, which results in the decrease of water permeance instead. Thus a maximum water permeance can be obtained as the CA weight ratio is at around 4.17 wt%.

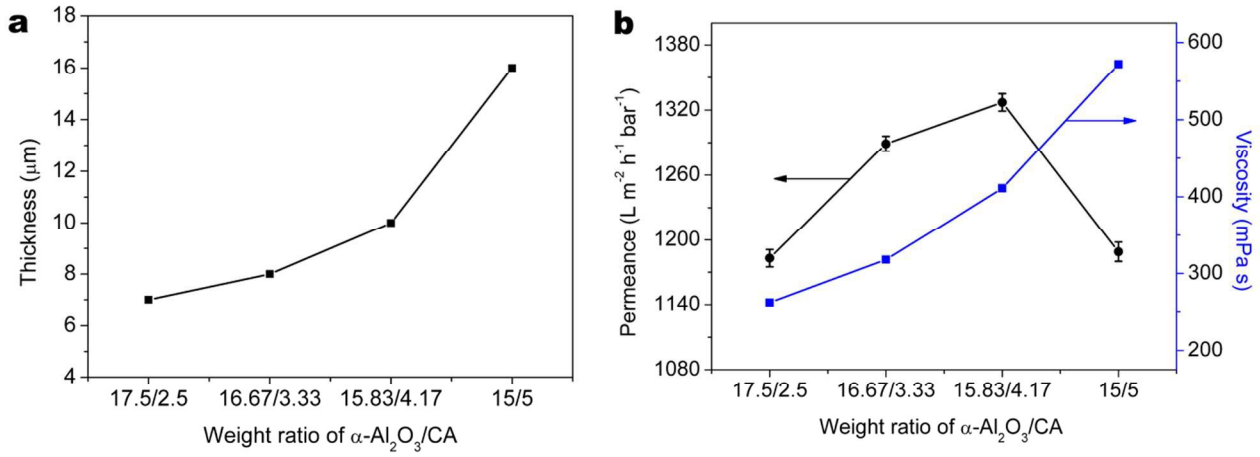

Fig. 7. Thickness and water permeance of the membranes prepared using slurries with different weight ratio of α-Al_2O_3/CA.

It is noted that when the similar technique reported in our previous work [22] was applied to prepare alumina membrane on the identical disc support, the membrane had an average pore size of 0.27 μm (Fig. 8a) and a water permeance of 673 L m^{-2} h^{-1} bar^{-1} (Fig. 8b), only half of that obtained via wet film phase inversion method. Fig. 8(d) shows the cross-sectional morphology of the membrane, no orientated microtubular pore structures were formed. Compared with the membrane made by the improved dip-coating process, the membrane prepared with wet film phase inversion method has a much higher permeability. In addition, the pure water permeances of ceramic membranes reported in the literatures are summarized in Table 1 for comparison with the present work. It can be found that both the average pore size and the membrane thickness are the important factors which affect the pure water permeance of the ceramic membrane. Compared with other ceramic membranes the membrane prepared by this technique has much better performances as well.

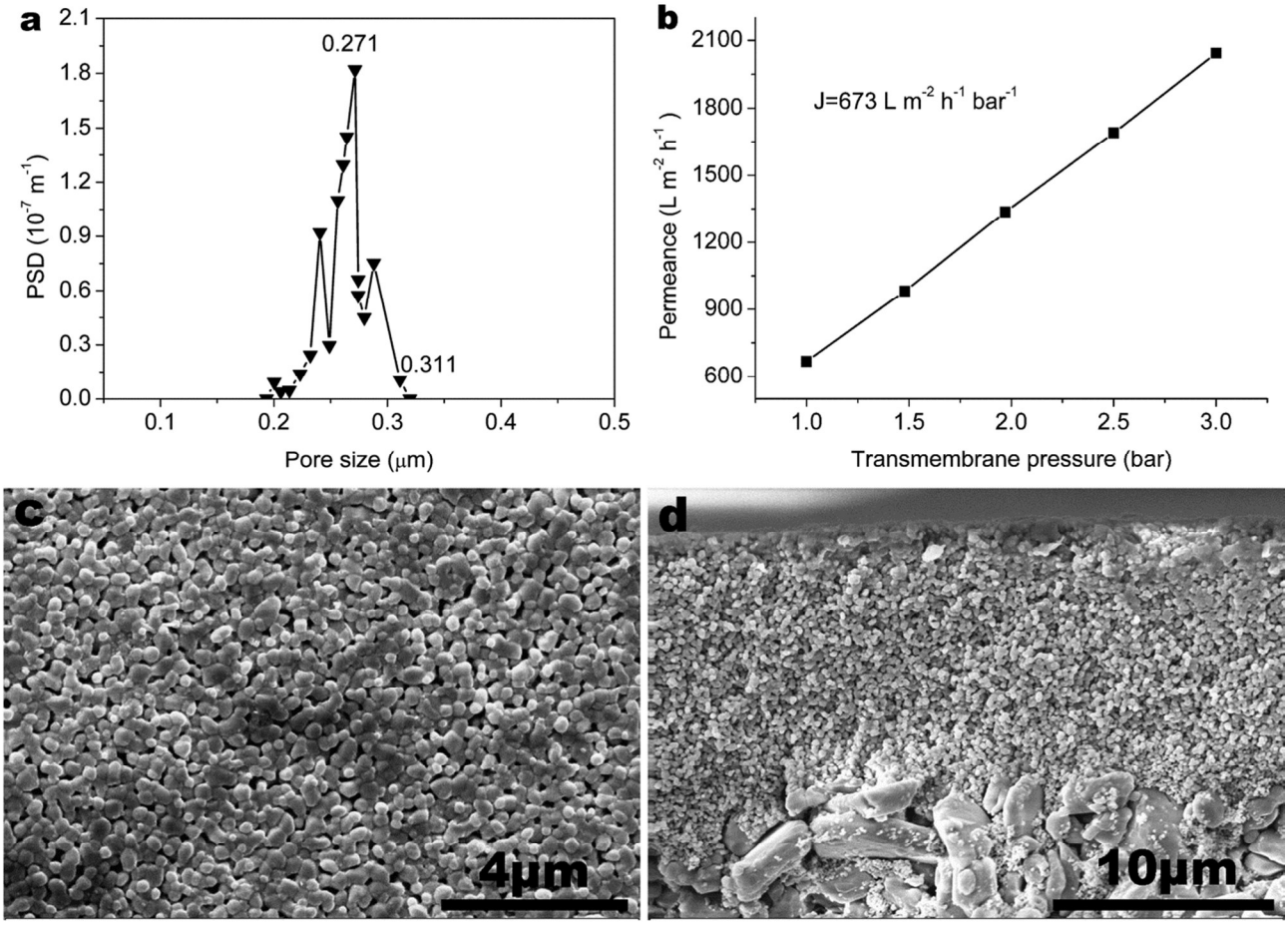

Fig. 8. Pore size distribution (a), water permeance (b), surface (c) and cross-sectional (d) morphologies of the alumina membrane prepared on the identical disc support via the similar technique. of the alumina membrane prepared on the identical disc support via traditional technique. [the slurry consists of 1.7 wt AOOH, 15.83 wt% α-Al_2O_3, 3.01 wt% PVA, 0.9 wt% PVP and 78.56 wt% H_2O].

Table 1. Comparisons pure water permeance of alumina membrane prepared in this work with those in other literatures.

Membrane material	Average pore size (μm)	Pure water flux (L m^{-2} h^{-1} bar^{-1})	Thickness (μm)	Reference
α-Al_2O_3	0.28	1.33×10^3	10	This work
ZrO_2	-	1×10^3	3 - 4	[31]
α-Al_2O_3	1.25	799	-	[18]
TiO_2	0.1	740	15 - 20	[32]
α-Al_2O_3	0.76	1.93×10^3	-	[12]
clay	0.18	867	-	[33]
Carbon	1.0	450.7		[34]

In conclusion, single-step preparation of highly permeable alumina membrane on the as-prepared macroporous ceramic support has been achieved by using the wet film phase inversion technique. The phase inversion of cellulose acetate dissolved in DMF results in the orientated microtubular pore structures with good connectivity and short pore length, which is conductive to decreasing of filtration resistance. The proper slurry viscosity effectively reduces the intrusion of membrane-forming particles into the support pores. This also contributes to increasing the membrane water permeance. The membrane prepared using the slurry with α-Al_2O_3/CA of 15.83/4.17 exhibits a narrow pore size distribution centered at about 0.28 μm and a water permeance of 1327 L m^{-2} h^{-1} bar^{-1}. Comparisons with other ceramic membranes shows that performances especially the water permeance of the membrane prepared with wet film phase inversion method has been improved greatly. The wet film phase inversion technique has demonstrated to be an efficient way to prepare

highly permeable ceramic membrane at low cost.

Acknowledgements

This work is financially supported by the National Natural Science Foundation of China (Grant No. 51472092) and Industry, Education and Academy Cooperation Project of Foshan City, Guangdong Province (Grant No. 2012HC100282).

References

1 J. Feng, Y. Fan, H. Qi and N. Xu, *J. Membr. Sci.*, 2007, **288**, 20-27.

2 T. Van Gestel, C. Vandecasteele, A. Buekenhoudt, C. Dotremont, J. Luyten, R. Leysen, B. Van der Bruggen and G. Maes, *J. Membr. Sci.*, 2002, **207**, 73-89.

3 V. T. Zaspalis, W. Van Praag, K. Keizer, J. R. H. Ross and A. J. Burggraaf, *J. Mater. Sci.*, 1992, **27**, 1023-1035.

4 W. Qin, C. Peng, M. Lv and J. Wu, *Ceram. Int.*, 2014, **40**, 13741-13746.

5 L. Zhu, Y. Dong, L. Li, J. Liu and S.-J. You, *RSC Adv.*, 2015, **5**, 11163-11174.

6 X. Wang, X. Tan, B. Meng, X. Zhang, Q. Liang, H. Pan and S. Liu, *RSC Adv.*, 2013, **3**, 4821-4834.

7 J.-F. Li, Z.-L. Xu, H. Yang, L.-Y. Yu and M. Liu, *Appl. Surf. Sci.*, 2009, **255**, 4725-4732.

8 H. A. Tsai, L. D. Li, K. R. Lee, Y. C. Wang, C. L. Li, J. Huang and J. Y. Lai, *J. Membr. Sci.*, 2000, **176**, 97-103.

9 D. Wang, W. K. Teo and K. Li, *J. Membr. Sci.*, 2002, **204**, 247-256.

10 S. Liu, K. Li and R. Hughes, *Ceram. Int.*, 2003, **29**, 875-881.

11 M. Lee, B. Wang, Z. T. Wu and K. Li, *J. Membr. Sci.*, 2015, **483**, 1-14.

12 Z. Shi, Y. Zhang, C. Cai, C. Zhang and X. Gu, *Ceram. Int.*, 2015, **41**, 1333-1339.

13 M. H. D. Othman, N. Droushiotis, Z. T. Wu, G. Kelsall and K. Li, *Adv. Mater.*, 2011, **23**, 2480-2483.

14 H. Wei, H. Hua, G. Jian-fen, L. Winnubst and C. Chu-sheng, *J. Membr. Sci.*, 2014, **452**, 294-299.

15 X. Tan, Y. Liu and K. Li, *Ind. Eng. Chem. Res.*, 2005, **44**, 61-66.

16 B. Wang and Z. Lai, *J. Membr. Sci.*, 2012, **405–406**, 275-283.

17 S. Xin, D. Dehua, G. Parkinson and L. Chun-Zhu, *J. Mater. Chem. A*, 2014, **2**, 410-417.

18 G. Xu, K. Wang, Z. Zhong, C.-s. Chen, P. A. Webley and H. Wang, *J.Mater. Chem. A*, 2014, **2**, 5841-5846.

19 B. F. K. Kingsbury and K. Li, *J. Membr. Sci.*, 2009, **328**, 134-140.

20 K. Li, X. Tan and Y. Liu, *J. Membr. Sci.*, 2006, **272**, 1-5.

21 C. C. Wei, O. Y. Chen, Y. Liu and K. Li, *J. Membr. Sci.*, 2008, **320**, 191-197.

22 W. Qin, K. Guan, B. Lei, Y. Liu, C. Peng and J. Wu, *J. Membr. Sci.*, 2015, **490**, 160-168.

23 M. Guglielmi, P. Colombo, F. Peron and L. Mancinelli Degli Esposti, *J. Mater. Sci.*, 1992, **27**, 5052-5056.

24 J. G. Wijmans, J. P. B. Baaij and C. A. Smolders, *J. Membr. Sci.*, 1983, **14**, 263-274.

25 J. H. Hao and S. Wang, *J. Appl. Polym. Sci.*, 1998, **68**, 1269-1276.

26 R. M. Boom, H. W. Reinders, H. H. W. Rolevink, T. van den Boomgaard and C. A. Smolders, *Macromolecules*, 1994, **27**, 2041-2044.

27 Y. Yip and A. J. McHugh, *J. Membr. Sci.*, 2006, **271**, 163-176.

28 C. A. Smolders, A. J. Reuvers, R. M. Boom and I. M. Wienk, *J. Membr. Sci.*, 1992, **73**, 259-275.

29 P. Wang, P. Huang, N. P. Xu, J. Shi and Y. S. Lin, *J. Membr. Sci.*, 1999, **155**, 309-314.

30 Y. F. Gu and G. Y. Meng, *J. Eur. Ceram. Soc.*, 1999, **19**, 1961-1966.

31 M. Qiu, Y. Fan and N. Xu, *J. Membr. Sci.*, 2010, **348**, 252-259.

32 Y. H. Wang, X. Q. Liu and G. Y. Meng, *Mater. Res. Bull.*, 2008, **43**, 1480-1491.

33 S. Khemakhem, A. Larbot and R. Ben Amar, *Ceram. Int.*, 2009, **35**, 55-61.

34 C. Song, T. Wang, Y. Pan and J. Qiu, *Sep. purif. technol*, 2006, **51**, 80-84.